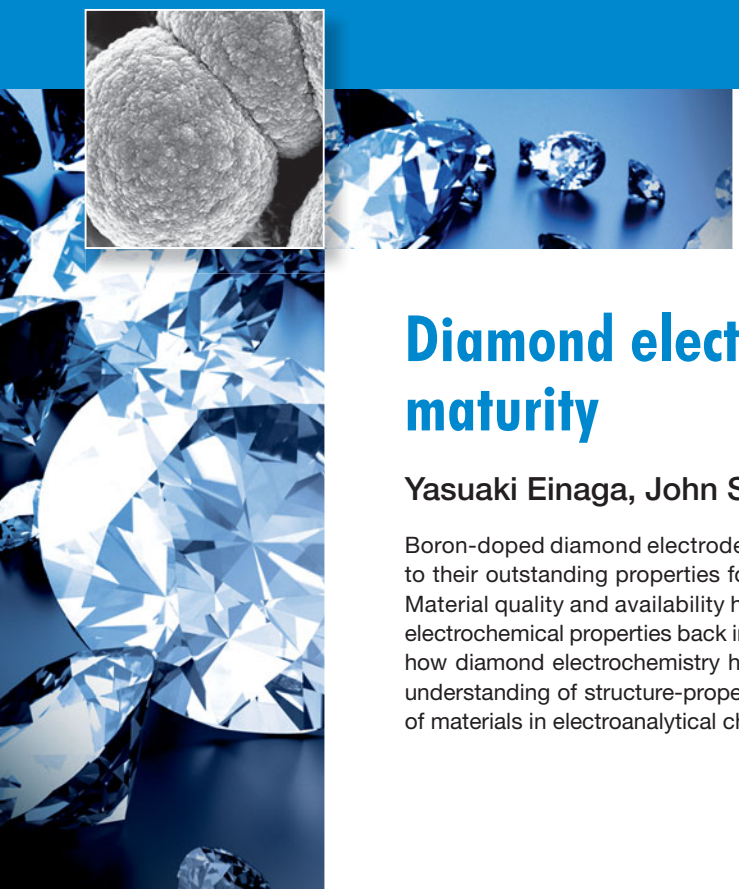


Diamond electrodes: Diversity and maturity

Yasuaki Einaga, John S. Foord, and Greg M. Swain

Boron-doped diamond electrodes have attracted increasing interest from researchers due to their outstanding properties for electroanalysis and other electrochemical applications. Material quality and availability have come a long way since the initial reports on the basic electrochemical properties back in the late 1980s and early 1990s. In this review, we highlight how diamond electrochemistry has diversified and matured in recent years in terms of the understanding of structure-property relationships and the development of new applications of materials in electroanalytical chemistry.

Introduction

Since the first publications on the basic electrochemical properties of diamond in the late 1980s and early 1990s,[1–3] as well as the first patent on the application of diamond anodes for treating wastewater prior to discharge into the environment,[4] interest in the use of electrically conducting diamond electrodes has steadily grown. Today, diamond electrodes find widespread use in electroanalysis, spectroelectrochemistry, neurochemistry (i.e., chemistry of neurotransmitters used for cellular communication), chemical/biological sensing, and water disinfection/purification.

Diamond electrodes have attracted this level of interest due to their excellent electrochemical properties.[5–10] These include (1) the ability to prepare the material in different architectures, (2) a wide working potential window, (3) enhanced signal-to-background ratios due to the low background current, (4) good activity without conventional pretreatment, (5) weak molecular adsorption, and (6) optical transparency. It could be argued that chemical vapor deposited (CVD) diamond is the most versatile of all the different carbon electrode materials because it can be used in electroanalysis to provide low detection limits for analytes with superb precision and stability,[11,12] for high-current density electrolysis (1–10 A/cm^2) in aggressive solution environments without any microstructural or morphological degradation,[13] as a corrosion-resistant electrocatalyst support,[14,15] and as an optically transparent electrode (visible and IR) for spectroelectrochemical measurements.[16–18]

This advanced carbon-based electrode provides researchers with a material that meets the requirements for a wide range of applications. In electroanalytical measurements, diamond electrodes generally provide significant improvements over conventional sp^2 carbon electrodes in terms of linear dynamic range, limit of detection, response precision, and response stability. Broad application of this novel electrode material has been somewhat limited until recent years because there were no commercial suppliers. Today, the situation has changed, as there are multiple commercial suppliers of electrically conducting diamond thin-film electrodes. Importantly, the cost of these materials is not high, as often perceived when one hears the word "diamond."

Diamond materials and electrode architectures

Several types of diamond electrodes can be prepared in different architectures. Single crystal diamond can be readily obtained and is most useful for fundamental studies of interfacial structure as well as grain boundary and crystallographic effects on rates of electrochemical reactions. Polycrystalline thin-film electrodes, deposited on properly pretreated substrates (e.g., Si, W, Mo, Nb, and Pt), are the most commonly utilized form of diamond. Sharpened metal wires can be coated with conducting diamond to form microelectrodes that are useful in

Yasuaki Einaga, Department of Chemistry, Keio University, Japan; einaga@chem.keio.ac.jp
John S. Foord, Department of Chemistry, Chemistry Research Laboratory, Oxford University, UK; john.foord@chem.ox.ac.uk
Greg M. Swain, Department of Chemistry, Michigan State University, USA; swain@chemistry.msu.edu
DOI: 10.1557/mrs.2014.94

© 2014 Materials Research Society

https://doi.org/10.1557/mrs.2014.94 Published online by Cambridge University Press

neuroscience, specifically for measurements of neurosignaling molecules in tissues or at single cells isolated in culture.

Diamond electrodes also can be patterned into microelectrode array structures (e.g., discs and bands). In electroanalytical measurements, microelectrode arrays offer several advantages over planar macroelectrodes, with one of the most important being the enhanced signal-to-background ratio. This is due to a higher rate of diffusional mass transport of an analyte to the small-dimension electrodes plus a lower background current from the reduced overall electrode area. Diamond microelectrode arrays are finding use as a platform for nerve cell growth, neural stimulation, and action potential monitoring for reading short duration changes in the membrane potential of an excitable cell.[19–21] In the future, these electrode arrays may find use for spatially resolved measurements of neurosignaling processes. More recently, electrically conducting diamond films with a high surface area have been prepared by coating substrate powders with a thin layer of ultrananocrystalline diamond (polycrystalline diamond grown from argon-rich source gas mixtures).[15,22] In this core–shell process, the excellent properties of diamond can be imparted to various substrate powders (e.g., diamond, glassy carbon, Ketjen Black [a type of electronconductive sp^2 carbon powder], metal oxides). Only recently have these materials begun to be studied and, in the future, they may find application as dimensionally stable electrodes for batteries and fuel cells or for chemical and biological sensing. In an effort to increase the specific surface area, work has also been done to fabricate nanostructured forms of diamond (cones and needles).[23,24] Examples of some of these different diamond architectures are presented in **Figure 1**a–e.

Three types of polycrystalline diamond can be deposited by microwave plasma-assisted CVD: microcrystalline (few μm grain size), nanocrystalline (NCD; <100 nm), and ultrananocrystalline (UNCD; <10 nm).[25] The conditions used to deposit diamond are specific to different reactor designs. For the conventional 1.5 kW ASTeX microwave system (now Seki Technotron), microcrystalline diamond films are routinely deposited from CH_4/H_2 source gas mixtures of 0.3–1.0%, microwave powers of 0.1–1 kW, gas pressures of 35–65 Torr, and substrate temperatures in the 700–850°C range. The microcrystalline films obtained from this widely used synthesis procedure are well-faceted, with crystallite dimensions on the order of a few micrometers or greater. The crystallites are randomly oriented, and there is significant twinning. Grain boundaries exist at the junctions between crystallites.

NCD and UNCD films are categorized based on their different growth chemistries and properties.[26–28] Structurally, UNCD films are distinct from their NCD counterparts, as

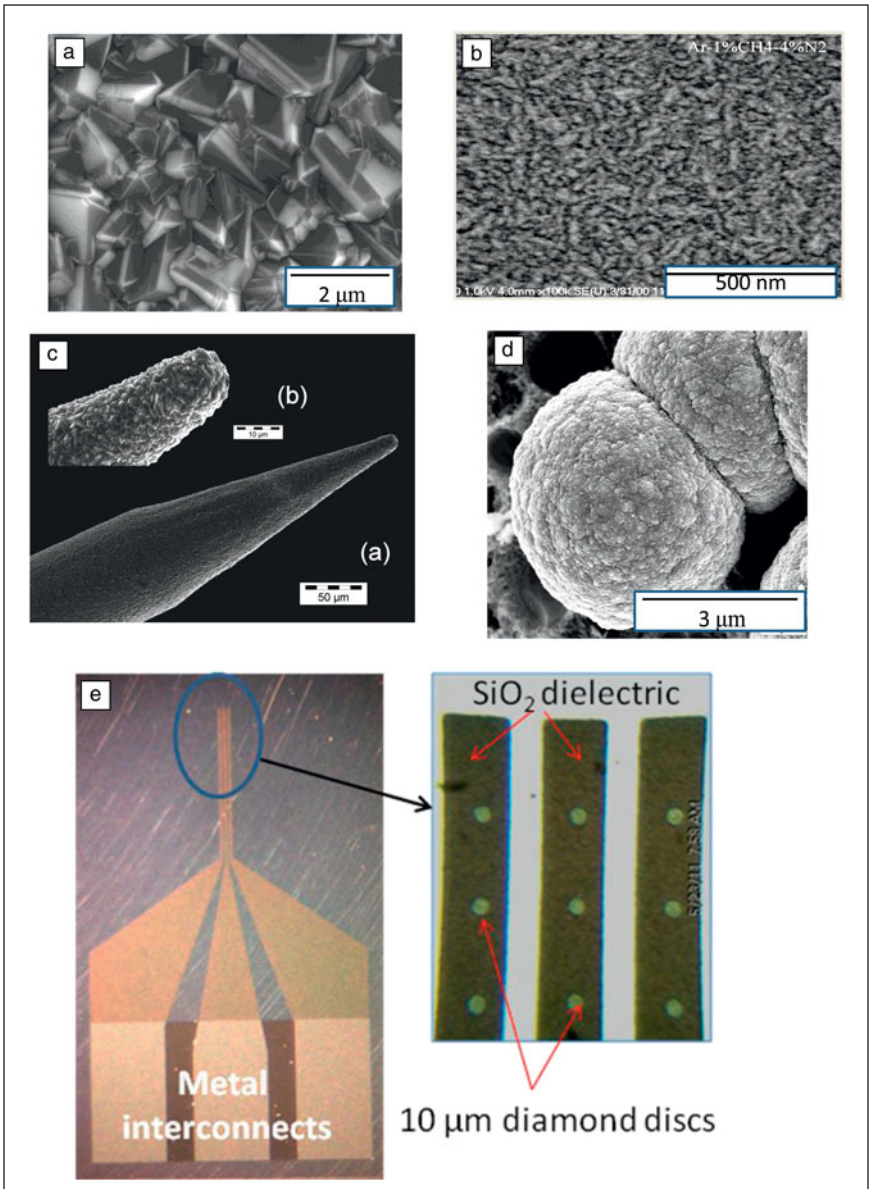


Figure 1. Scanning electron microscope images of (a) a boron-doped microcrystalline diamond film grown from a 1% CH_4/99% H_2 source gas mixture with B_2H_6 added for doping (scale bar = 2 μm). (b) A nitrogen-incorporated ultrananocrystalline diamond film grown from a 1% CH_4/4% N_2/95% Ar source gas mixture. (c) A sharpened Pt wire overcoated with a boron-doped diamond film grown from a 1% CH_4/99% H_2 source gas mixture with B_2H_6 added for doping.[70] (d) Glass carbon powder particles overcoated with a layer of boron-doped ultrananocrystalline diamond grown from a 1% CH_4/5% H_2/94% Ar with B_2H_6 added for doping (two particles fused together in image, see Reference 22). (e, left) 2 μm diameter glass carbon powder particles overcoated with a layer of boron-doped ultrananocrystalline diamond grown from a 1% CH_4/5% H_2/94% Ar with B_2H_6 added for doping (two particles fused together in image).[22] (e, right) Diamond microelectrode array consisting of three rows of 10 μm diamond electrodes isolated by a SiO_2 dielectric layer. The array was prepared by Michael Becker of the Fraunhofer Center for Coatings and Laser Applications at Michigan State University.

https://doi.org/10.1557/mrs.2014.94 Published online by Cambridge University Press

the former possess a smaller grain size, more grain boundaries, and sp^2-bonded carbon atoms in these grain boundaries. Various groups have reported on the structural and electrochemical properties of nitrogen-incorporated and boron-doped UNCD,[27,29,30] as well as boron-doped NCD.[27] For the most part, many of the basic electrochemical properties of NCD and UNCD are similar.

In order to have sufficient electrical conductivity for most electrochemical measurements (< 0.1 ohm•cm or > 10 S/cm), diamond films must be doped with boron (boron-doped diamond, BDD), generally at a concentration of ~10^{20} cm^{-3} or greater, as this is the most practical dopant to date. It should be pointed out that there is ongoing research with alternate dopants such as nitrogen,[31] phosphorous,[32] and sulfur.[33,34] Boron is added to the source gas mixture using B_2H_6 (diborane) or $B(CH_3)_3$ (trimethylboron). The films are rendered electrically conducting through incorporation of boron dopant atoms during deposition, although the electrical conductivity depends in a complex manner on lattice hydrogen, defects, and dangling bonds, in addition to the doping level. The interaction between electronic levels of boron and the formation of a boron impurity band starts in the 10^{18} cm^{-3} boron doping range.[35] At these doping levels, the diamond films exhibit semiconducting electrical properties. Metallic conductivity is observed starting around 3×10^{20} cm^{-3}.[36] In fact, films can be doped as high as 10^{21} B/cm^3. Such films have electrical resistivities on the order of ~0.001 Ω•cm.[37] An additional graphitic phase can sometimes appear in heavily boron-doped films. Importantly though, in polycrystalline films, the boron doping is non-uniform, as the dopant incorporation strongly depends on the growth sector.[38,39] This heterogeneous doping has been confirmed by Raman measurements,[40,41] conducting probe atomic force microscopy, and scanning electrochemical microscopy.[42,43] Recent transmission electron microscopy and electron energy-loss spectroscopy work has shown that boron is incorporated into the defect regions of the diamond grains.[44] Importantly, the heterogeneous doping can cause non-uniform electrical and electrochemical properties across a film surface.

Several factors influence the diamond thin-film electrode response (i.e., electrode reaction kinetics): (1) potential-dependent density of electronic states, which is affected by the doping type, level, and distribution, (2) surface chemistry, (3) morphology and microstructure, (4) defect density, (5) non-diamond carbon impurity content, and (6) double layer structure.[45–47] The extent to which any of these factors affects the electrode response very much depends on the reaction mechanism for the particular redox system under study. Importantly, these properties can all be controlled by selection of the appropriate deposition conditions. The deposition conditions and film growth procedures can vary from lab to lab, which can affect the resulting film quality and electrode properties. For example, differences in substrate pretreatment prior to growth, source gas composition used during growth, the cool-down procedure after growth, and postgrowth chemical treatment (e.g., acid washing) could lead to variability in electrode properties and performance.

Here, we highlight how the field of "diamond electrochemistry" has diversified and matured in recent years in terms of the understanding of structure-property relationships and the development of new applications of the material in electroanalytical chemistry. Specifically, we (1) discuss how two material properties, the boron-doping level and the sp^2 carbon impurity content, affect the basic electrochemical response of polycrystalline diamond thin-film electrodes, (2) highlight some recent electroanalytical applications of the material, and (3) show how diamond prepared in the form of microelectrodes can be used to study neurosignaling processes *in vitro* in the peripheral nervous system as an example demonstrating the possibilities of diamond electrodes.

Dependence of the electrochemical response on the boron-doping level and sp^2-bonded carbon impurity content

Two factors that influence the performance/response of polycrystalline diamond thin-film electrodes are the (1) boron-doping level and (2) adventitious sp^2-bonded carbon impurity. The primary effect of the doping level is on the electrode's electrical conductivity, and this affects the response for every redox analyte. For most electrochemical applications, one desires highly conducting diamond films. The higher the doping level, the higher the carrier concentration (holes), and the higher the electrical conductivity. More subtle effects on the film morphology and composition can also occur. For example, as the boron content in a film increases, the size of the crystallites decreases. Additionally, a sp^2 carbon impurity phase appears at very high boron doping levels.[48] In terms of the effect of the non-diamond sp^2 carbon, the voltammetric background current increases, the working potential window decreases, and molecular adsorption increases with increasing impurity content.[47] Additionally, the presence of this adventitious impurity affects the electron-transfer kinetics of redox systems differently. For some redox systems, the presence of the impurity strongly accelerates the heterogeneous rate of electron-transfer (e.g., oxygen reduction), while for others, the impurity has little effect on the kinetics (e.g., $Ru(NH_3)_6^{+3/+2}$).[47]

For electrochemical detection, the wide potential window and low background current characteristics of polycrystalline diamond electrodes enable highly sensitive detection of various chemical species. As an example, three BDD electrodes (BDD-A, B, and C) with various boron concentrations (albeit a narrow range of doping levels) were prepared. Two of these films (BDD-A and B) had negligible sp^2 carbon impurity, while one (BDD-C) had a relatively high sp^2 carbon impurity content (**Table I**).[49]

Figure 2 shows cyclic voltammetric curves for these different diamond electrodes in (a) a supporting electrolyte solution and in (b) equimolar amounts of $Fe(CN)_6^{3-}$ and $Fe(CN)_6^{4-}$ in KCl. Data for a glassy carbon electrode are also presented for comparison.[49] It can be seen that the voltammetric background

https://doi.org/10.1557/mrs.2014.94 Published online by Cambridge University Press

Table I. Gas phase composition and boron-doping level for a series of highly boron-doped diamond electrodes.[49]

Electrode	B/C ratio in the gas phase (%)	[B] in diamond (cm^{-3})	G-band (1520 cm^{-1}) in Raman spectrum
BDD-A	0.5	2×10^{21} (1.1 at.%)	Not observed
BDD-B	1	4×10^{21} (2.3 at.%)	Not observed
BDD-C	5	5.5×10^{21} (3.1 at.%)	Observed

BDD, boron-doped diamond.

current and the working potential window are affected by the boron-doping level even over this narrow range. BDD-A exhibits a low background current (significantly lower than glassy carbon) and wide working potential window (~3 V) characteristic of high-quality polycrystalline diamond.[1–3,5–10,50] The highest doped film exhibits the largest background current and most narrow potential window, both comparable to glassy carbon (Figure 2a). This is also the film that has sp^2 carbon impurity at the surface. In fact, the synthesis conditions (C/H ratio in the carrier gas, gas flow rate, and temperature) for the three electrodes were identical in the experiments. Only the B/C mixing ratio was varied. The highest B/C ratio (BDD-C) produced some sp^2 carbon impurities on the surface. Comparing the curves for BDD-A and C, which are films with comparable doping magnitudes, one can see that the surface sp^2 carbon impurities have a significant effect on the electrode response in terms of increased background current and decreased potential window.[49,50] The trends in the background voltammetric curves reveal how useful electrochemical measurements can be at assessing diamond film quality.

Figure 2b shows voltammetric curves for the $Fe(CN)_6^{3-/4-}$ redox system for the different diamond films. The electrodes were anodically pretreated prior to the measurements by applying 1 mA/cm^2 for 10 min. This produces an oxygen-terminated surface.[51,52] As-deposited diamond normally possesses a hydrogen-terminated, hydrophobic surface due to growth in the hydrogen-rich atmosphere. However, the surface is easily converted to a hydrophilic, oxygen-terminated one by chemical or electrochemical oxidation. Two peaks are seen, one on the forward scan (positive potential direction) at *ca.* 0.30 V for the one-electron oxidation of $Fe(CN)_6^{4-}$ to $Fe(CN)_6^{3-}$, and one on the reverse scan (negative potential direction) at *ca.* 0.23 V for the one-electron reduction of $Fe(CN)_6^{3-}$ back to $Fe(CN)_6^{4-}$.

ΔE_p (E_p^{ox}–E_p^{red}) is a useful diagnostic that can be related to the heterogeneous electron-transfer rate constant for the redox system if ohmic resistance effects from the electrolyte solution and electrode are negligible. Generally speaking, for a diffusion-controlled process, the smaller the ΔE_p (closer to the theoretical limit of ~59 mV for a 1-electron redox reaction), the larger the rate constant, and the faster the rate of electron transfer. It can be seen in Figure 2b that unlike the background voltammetric curves, ΔE_p for this redox system is largely independent of the doping level over this narrow range as well as the presence of the sp^2 carbon impurity. While there is some variation in peak current magnitude, ΔE_p for the different diamond electrodes is similar to the value for activated glassy carbon. This indicates that the rate of electron transfer for this redox system, under these conditions, is similar for all of the diamond electrodes and comparable to that for glassy carbon.

$Fe(CN)_6^{3-/4-}$ is well known to be a surface-sensitive redox system at diamond and sp^2 carbon electrodes.[46,53,54] For example, it has been shown that ΔE_p for $Fe(CN)_6^{3-/4-}$ is relatively independent of the sp^2 carbon impurity but highly dependent on the surface chemistry of diamond electrodes.[46,53] ΔE_p has been shown to increase at diamond electrodes with increasing surface oxygen coverage. This trend reveals more sluggish electron-transfer kinetics for the oxygen-terminated electrode as compared to the hydrogen-terminated electrode.[46,53] This trend can be reversed simply by rehydrogenating the surface in a hydrogen microwave plasma. It would appear, based on the data in Figure 2b, that the surface chemistry effects on the kinetics of this redox system depend on the boron-doping level of the film (i.e., the effects are less evident for more heavily doped films). The take-home message is that in order to optimally apply diamond electrodes for electrochemical detection and sensing, it is important to understand how the doping level, adventitious sp^2 carbon impurity, and surface chemistry affect the redox reaction kinetics for the particular analyte species under study.

Other electrode characteristics that are important in electroanalysis are the background current magnitude and noise (fluctuations in the background current) in electrode displays, which can mask the target analyte's electrochemical signal and, as a consequence, ultimately control

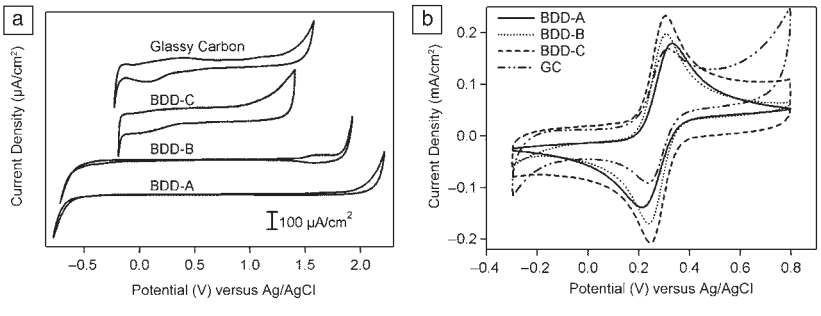


Figure 2. (a) Background cyclic voltammetry (I-E) curves in 0.5 M H_2SO_4 for boron-doped diamond (BDD)-A, BDD-B, BDD-C, and glassy carbon electrodes. Scan rate 100 mV/s. (b) Cyclic voltammetry (I-E) curves for 0.5 mM $[Fe(CN)_6]^{3-}$ and 0.5 mM $[Fe(CN)_6]^{4-}$ in 1 M KCl at BDD-A, BDD-B, BDD-C, and glassy carbon (GC) electrodes. Scan rate 100 mV/s.[49]

https://doi.org/10.1557/mrs.2014.94 Published online by Cambridge University Press

the limit of detection (LOD). The LOD is the minimum concentration of an analyte detectable, usually at a signal-to-noise ratio of 3 or greater. The background voltammetric current has various distinct origins. When the electrode potential is scanned during a measurement, a capacitive current due to the electrochemical double layer at the interface arises. In addition, materials such as glassy carbon tend to have a significant coverage of redox-active carbon-oxygen functional groups on the surface.[55,56] For example, the quinone/hydroquinone couple is a typical surface functionality. These functional groups contribute a Faradaic current component as well. An important advantage of diamond is that the background current tends to be low, especially for higher-phase purity materials, leading to lower detection limits. The low background current typical of diamond results from a lower capacitance than glassy carbon (~5 versus ~30 μF/cm^2) and the absence of significant quantities of electroactive surface carbon-oxygen functionalities.[2,6,7,50,56]

Some recent electroanalytical applications

An important application of electrochemistry is the field of electroanalysis, which relates to the use of electrochemistry to determine the concentration of chemical species in a sample. Compared to many analytical techniques, electrochemical methods normally involve relatively low cost and highly portable instrumentation, so they are suitable for real-time monitoring in the field. Furthermore, electrochemical methods generally offer high sensitivity, low detection limits, and wide dynamic range, and can readily be miniaturized to achieve excellent spatial sensitivity, for example in probing living organisms. Perhaps the best-known example of electroanalysis is the blood glucose sensor.[57,58] Electrochemical sensors have been and continue to be used in a number of areas, for example, the detection of CO,[59] *in vivo* monitoring of bioactive species,[60] and environmental detection of heavy metals[61] and organic pollutants.[62]

Electroanalytical sensors frequently utilize voltammetric techniques, which encompass the measurement of current-voltage relationships associated with the oxidation or reduction of the target analyte at the electrode surface. Properties of the electrode have a profound influence on the observed response, as mentioned previously, and it is here that the unique properties of boron-doped diamond can be exploited. One general requirement for electroanalysis is that the target analyte be electroactive within the potential range defined by the values at which the solvent, most commonly water, is oxidized and reduced. For a catalytic electrode like Pt, this accessible range in water is practically limited to about 1.2 V. Importantly for diamond electrodes, kinetic limitations associated with water electrolysis can usefully broaden the accessible potential range to >3 V,[1–3,5–10,50,63] which is vital for the detection of analytes that are oxidized at high positive potentials. A typical example showing how this can be exploited is the use of diamond electrodes for the analysis of the active ingredients in pharmaceutical preparations. Some representative voltammetric data are shown in **Figure 3**, revealing distinct electrochemical currents associated with the oxidation of paracetamol (pain relief; 0.75 V), caffeine (1.37 V), and orphenadrine (blocks the neurotransmitter acetylcholine [e.g., used to treat muscle spasms]; 1.60 V) with good linearity in the 100 nM–60 μM range.[64] The ability to use diamond electrodes at high potentials is key to this type of application.

A multitude of surface functionalization strategies have been developed for diamond, and generally they all yield a relatively stable surface chemistry. This can be exploited to tune the electrode activity to suit a particular application. Surface functionalization can be beneficial for electroanalysis by promoting specific interactions with the target analyte that lowers the activation barrier for electron transfer. Surface functionalization can also be beneficial by prohibiting strong site-blocking interactions of an analyte or a reaction product with the electrode, which would normally lead to electrode fouling.

A potential problem in electroanalysis is the electrode passivation that can occur due to the undesired adsorption of chemical species from solution. This adsorption causes electrode response attenuation referred to as fouling. Diamond electrodes naturally exhibit a high resistance to fouling due to the sp^3-bonded carbon microstructure, the absence of an extended π-electron system, like that which exists in graphitic carbons, and the relative non-polar nature of the hydrogen-terminated surface.[50,65]

The easiest-to-achieve surface functionalizations include hydrogen termination, which produces a strongly hydrophobic surface, and the "oxidized" termination, which produces a surface with hydrophilic character.[46,66] For example, the electrochemical detection of an important class of environmental pollutants known as endocrine disruptors using diamond

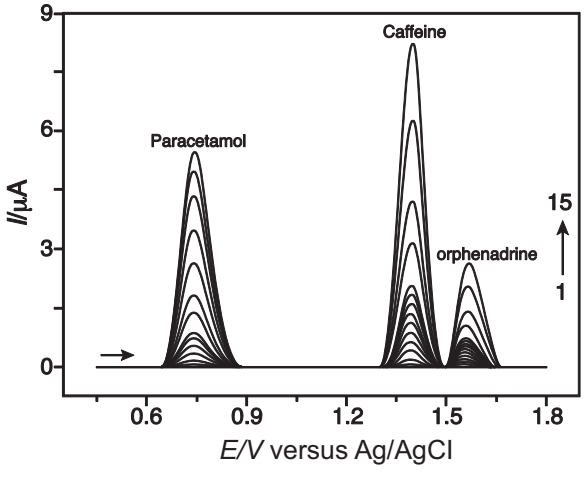


Figure 3. Square-wave voltammograms showing the oxidation waves seen from paracetamol (0.75 V), caffeine (1.37 V), and orphenadrine (1.6 V) mixtures in dilute sulphuric acid at a boron-doped diamond electrode for a range of increasing concentrations (scans 1–15). Reproduced with permission from Reference 64. © 2013 Wiley.

https://doi.org/10.1557/mrs.2014.94 Published online by Cambridge University Press

electrodes has been studied.[67] These compounds interfere with the endocrine system in mammals causing a range of health disorders. Whereas these analytes, and potentially their reaction products, adsorb strongly at practically all electrodes, resulting in electrode passivation and poor detection figures of merit, negligible adsorption was observed at oxygen-terminated diamond, resulting in a wide linear detection range up to 100 μM. Conversely, if the diamond electrode was hydrogen-terminated, strong adsorption could be promoted, enabling the investigation of the low concentration range by adsorptive voltammetry.[67]

This ability to produce a stable surface chemical modification of diamond also enables the construction of high performance, high selectivity electrode sensors, for example, for the detection of specific oligonucleotide sequences in DNA analysis.[68] As shown in **Figure 4**, arrays of oligonucleotides can be stably grafted to the diamond surface. These can then selectively bind with the complementary oligonucleotide from solution, an event that can be detected sensitively using electrochemical methods.[68] In Figure 4, this is illustrated for the detection of a cancer marker, CK20. The key to the success of this approach is the unusually stable surface functionalization that can be achieved on diamond. The present example clearly opens up a new approach to next-generation electrochemical gene sensor platforms.

In vitro electrochemistry

An emerging application of diamond electrodes is in the area of neuroscience. Small-sized microelectrodes (micrometers in dimension, or smaller) are needed for these measurements. They can be prepared by coating a conducting diamond film on a sharpened metal wire, typically W[69] or Pt.[70] Electrochemical methods provide exquisite details about dynamic changes in the concentration of an electroactive neurosignaling molecule near its site(s) of release and action. What is needed for these measurements is an electrode with a response that is unaffected by the complex biological (tissue) environment. Diamond meets this requirement. Changes in local concentration of a neurotransmitter can be recorded as an oxidation or reduction current. The measured current is proportional to the concentration of an electroactive species in the extracellular space near the electrode. A body of literature now exists showing that diamond microelectrodes[71] can be used to sensitively, reproducibly, and stably measure (1) norepinephrine (NE) release from sympathetic nerves, which is important for regulating the diameter of arteries and veins (i.e., vascular tone)[72] and (2) serotonin release from enterochromaffin cells lining the mucosa of the small and large intestine, which is an important first-step in propulsion of intestinal content.[73]

Figure 5 demonstrates the concept of continuous amperometric monitoring of NE release from sympathetic nerves that supply blood vessels. Through the release of NE and/or ATP, these nerves play a critical role in controlling the diameter of blood vessels. Abnormalities in these regulatory processes are associated with hypertension.[74] The stable surface microstructure of diamond at the positive detection potentials and its resistance to molecular adsorption in the complex tissue environment (i.e., electrode fouling) make these measurements possible. The innervating nerve fibers and localized storage areas for the vasoconstricting NE are depicted in the drawing by the solid circles (varicosities or storage sites) connected by the solid lines (nerve fibers). The diamond microelectrode is positioned against the blood vessel surface. NE released from multiple nearby storage sites is detected via a two-electron, two-proton oxidation reaction that is shown in the lower right of the figure.

Lower left in Figure 5 shows an oxidation current-time curve of a typical measurement. A few details are warranted about the curve shape. The current increases from the baseline level, due to the electrically evoked release of NE, reaches a maximum, and then decays back to the baseline after the release ceases. The measured oxidation current is related to the time-dependent flux ($\Delta C/\Delta x$) of NE to the diamond microelectrode. ΔC is the NE concentration difference between the sites of release and the electrode surface. Since a detection potential is selected at which the current is limited by mass transport, the surface concentration of NE is effectively zero at all times. The parameter, Δx, is the distance from the release sites to the microelectrode, which remains constant during a measurement. Therefore, it is the change in NE concentration in the extracellular space that affects the measured current. In *in vitro* measurements at blood vessel surfaces, Δx is kept constant by placing the

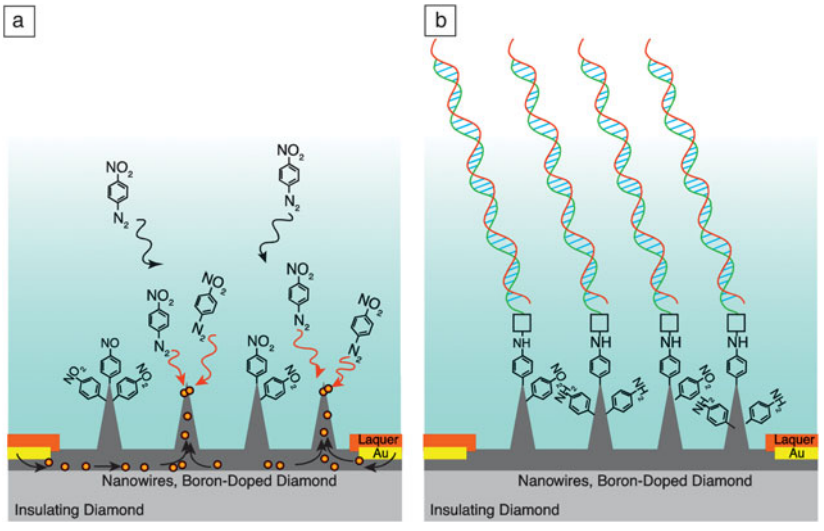


Figure 4. (a) Schematic of the electrochemical attachment of a phenyl linker molecule to a diamond electrode exhibiting a nanowire morphology, which is subsequently used to bind single-stranded oligonucleotide probe molecules. (b) Binding of CK20 cancer marker DNA to the oligonucleotide probe modifies the interface and can be detected electrochemically. Reproduced with permission from Reference 68. © 2009 Elsevier.

https://doi.org/10.1557/mrs.2014.94 Published online by Cambridge University Press

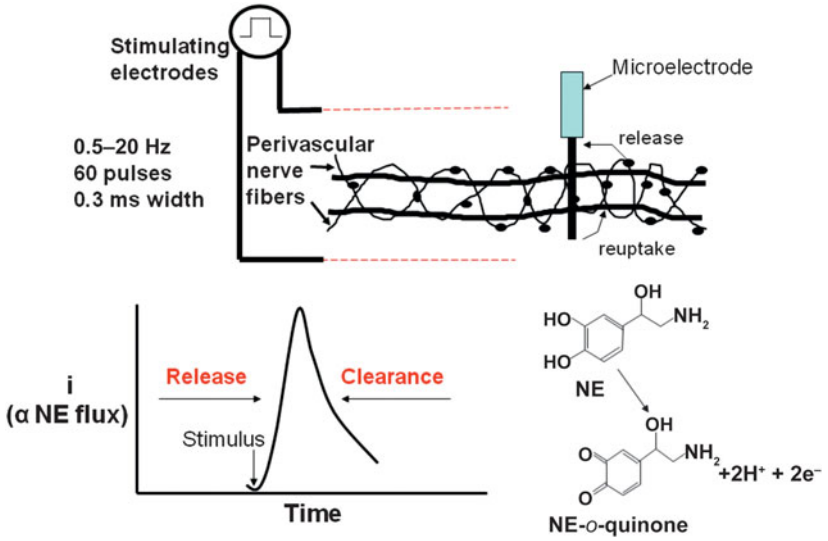


Figure 5. Concept of the *in vitro* measurement of electrically evoked norepinephrine (NE) release from sympathetic nerves supplying blood vessels using a diamond microelectrode (top). Dynamic changes in neurotransmitter concentration at the blood vessel surface are measured as an oxidation current using continuous amperometry (lower left). The redox reaction mechanism for NE is shown (lower right). The concept and use of diamond microelectrodes for this measurement have been reported elsewhere.[72,74]

recording microelectrode against the vessel. If this is done with a bit of tension, then the microelectrode will move with the vessel as it contracts and relaxes.[72,74]

The time-dependent NE flux to the diamond microelectrode is influenced in a complex manner by several processes: the number of neurotransmitter molecules released from nearby sites offset by (1) the inhibition of release through activation of prejunctional autoreceptors and (2) clearance by the prejunctional norepinephrine reuptake transporter (NET).[74] A large fraction of the NE molecules released will be quickly cleared from the extracellular space by NET and not be detected. Therefore, release in combination with autoinhibition and reuptake dynamically affect ΔC. This is reflected in the current-time trace in Figure 5. Immediately after stimulation, the current rises quickly as the NE flux at the microelectrode surface increases. Shortly after release and at the end of the stimulus, ΔC reaches a maximum. Activation of the prejunctional autoreceptors by excreted NE turns off the release process. At this point, the flux becomes controlled by NET. Clearance by NET causes the NE flux to progressively decrease, as reflected by the decreased current. The peak current or the peak charge can be used as a measure of NE in the extracellular space. These measurements, which typically take a couple of hours to complete, can be made with diamond in arteries and veins from rats, mice, and humans. Diamond is clearly an enabling material for these measurements, as the material provides superb response sensitivity, reproducibility, and stability.[72,74]

Conclusion

Boron-doped diamond is now a well-developed and mature electrode material. New applications of the material for a variety of chemical and bioanalyte species continue to emerge. A diverse array of diamond electrode architectures is available, many of these commercially, for use in multiple electrochemical applications, including electroanalysis, spectroelectrochemistry, neurochemistry, chem/biosensing, and water disinfection/purification. For electroanalysis, diamond generally outperforms other carbon electrode materials in terms of response sensitivity, response precision, limit of detection, and response stability. Several properties influence the diamond electrode response for a redox analyte, the degree to which very much depends on the particular analyte. In order to realize the best diamond electrode performance for an electrochemical application, appropriate electrode properties must be obtained through control over the boron doping level, the sp^2 carbon impurity content, and the surface termination.

Acknowledgments

Y.E. acknowledges JST-CREST for research support. He also thanks T. Watanabe for performing experiments and for fruitful discussions. J.S.F. acknowledges the Engineering and Physical Science Research Council and the EU INT "Matcon" for financial support. G.M.S. would like to thank the National Science Foundation (CHE-0911383), the National Institutes of Health (P01HL070687), and the Army Research Office (W911NF-14–0063) for financial support for different aspects of the diamond electrode research in recent years. The significant contributions of Drs. Jinwoo Park, Hua Dong, and James J. Galligan to the *in vitro* electrochemical measurements are hereby recognized.

References

1. Y.V. Pleskov, A.Y. Sakharova, M.D. Krotova, L.L. Bouillov, B.V. Spitsyn, *J. Electroanal. Chem.* **228**, 19 (1987).
2. G.M. Swain, R. Ramesham, *Anal. Chem.* **65**, 345 (1993).
3. R. Tenne, K. Patel, K. Hashimoto, A. Fujishima, *J. Electroanal. Chem.* **347**, 409 (1993).
4. J.J. Carey, J.C.S. Christ, S.N. Lowery, US Patent 5,399,246 (1995).
5. H.B. Martin, A. Argoitia, U. Landau, A.B. Anderson, J.C. Angus, *J. Electrochem. Soc.* **143**, L133 (1996).
6. G.M. Swain, in *Electroanalytical Chemistry*, A.J. Bard, I. Rubinstein, Eds. (Marcel Dekker, NY, 2004), vol. **22**, pp. 182–277.
7. A. Fujishima, Y. Einaga, T.N. Rao, D.A. Tryk, Eds., *Diamond Electrochemistry* (BKC Inc. and Elsevier, Amsterdam, 2005).
8. A. Kraft, *Int. J. Electrochem. Sci.* **2**, 355 (2007).
9. J.H. Luong, K.B. Male, J.D. Glennon, *Analyst* **134**, 1965 (2009).
10. E. Brillas, C.A. Martinez-Huitle, Eds., *Synthetic Diamond Films* (Wiley, NY, 2011).
11. J. Xu, G.M. Swain, *Anal. Chem.* **70**, 1502 (1998).
12. T.A. Ivandini, T.N. Rao, A. Fujishima, Y. Einaga, *Anal. Chem.* **78**, 3467 (2006).
13. J. Wang, G.M. Swain, *Electrochem. Solid-State Lett.* **5**, E4 (2002).
14. L. LaTorre Riveros, D.A. Tryk, C.R. Cabrera, *Rev. Adv. Mater. Sci.* **10**, 256 (2005).
15. L. Guo, V.M. Swope, B. Merzougui, G.M. Swain, *J. Electrochem. Soc.* **157**, A19 (2010).
16. J. Stotter, J. Zak, Z. Behler, Y. Show, G.M. Swain, *Anal. Chem.* **74**, 5924 (2002).

https://doi.org/10.1557/mrs.2014.94 Published online by Cambridge University Press

17. H.B. Martin, P.W. Morrison Jr., *Electrochem. Solid-State Lett.* **4**, E17 (2001).
18. Y. Dai, D.A. Proshlyakov, J.K. Zak, G.M. Swain, *Anal. Chem.* **79**, 7526 (2007).
19. M. Bonnauron, S. Saada, L. Rousseau, G. Lissorgues, C. Mer, P. Bergonzo, *Diam. Relat. Mater.* **17**, 1399 (2008).
20. R. Kiran, L. Rousseau, G. Lissorgues, E. Scorsone, A. Bongrain, B. Yvert, S. Picaud, P. Mailley, P. Bergonzo, *Sensors* **12**, 7669 (2012).
21. V. Maybeck, R. Edgington, A. Bongrain, J.O. Welch, E. Scorsone, P. Bergonzo, R.B. Jackman, A. Offenhausser, *Adv. Healthc. Mater.* **3**, 283 (2014).
22. D.Y. Kim, B. Merzougui, G.M. Swain, *Chem. Mater.* **21**, 2705 (2009).
23. D. Luo, L. Wu, J. Zhi, *ACS Nano* **3**, 2121 (2009).
24. J. Hees, R. Hoffmann, A. Kriele, W. Smirnov, H. Obloh, K. Glorer, B. Raynor, R. Driad, N. Yang, O.A. Williams, C.E. Nebel, *ACS Nano* **26**, 3339 (2011).
25. O.A. Williams, *Diam. Relat. Mater.* **20**, 621 (2011).
26. J.E. Butler, A.V. Sumant, *Chem. Vapor Depos.* **14**, 145 (2008).
27. S. Wang, V.M. Swope, J.E. Butler, T. Feygelson, G.M. Swain, *Diam. Relat. Mater.* **18**, 669 (2009).
28. D.M. Gruen, *MRS Bull.* **23**, 32 (1998).
29. Q. Chen, D.M. Gruen, A.R. Krauss, T.D. Corrigan, M. Witek, G.M. Swain, *J. Electrochem. Soc.* **148**, E44 (2001).
30. Y. Show, M.A. Witek, P. Sonthalia, D.M. Gruen, G.M. Swain, *Chem. Mater.* **15**, 879 (2003).
31. N. Neugebohrn, T. Sun, F.A.M. Koech, G.C. Hembree, R.J. Nemanich, T. Schmidt, J. Falta, *Diam. Relat. Mater.* **4**, 12 (2013).
32. A. Lazea, V. Mortet, I. D'Haen, P. Geithner, J. Ristein, M. D'Olieslaeger, K. Haenen, *Chem. Phys. Lett.* **454**, 310 (2008).
33. G. Morell, A. Gonzalez-Berrios, B.R. Weiner, S. Gupta, *J. Mater. Sci. Mater. Electron.* **17**, 443 (2006).
34. F.A.M. Koeck, R.J. Nemanich, *Diam. Relat. Mater.* **15**, 2006 (2006).
35. E. Gheeraert, A. Deneuville, J. Mambou, *Diam. Relat. Mater.* **7**, 1509 (1998).
36. J.P. Lagrange, A. Deneuville, E. Gheeraert, *Diamond Relat. Mater.* **7**, 1390 (1998).
37. K. Nishimura, K. Das, J.T. Glass, *J. Appl. Phys.* **668**, 3142 (1991).
38. E. Gheeraert, P. Gonon, A. Deneuville, L. Abello, G. Lucazeau, *Diam. Relat. Mater.* **2**, 742 (1993).
39. K. Ushizawa, K. Watanabe, T. Ando, I. Sakaguchi, M. Nishitani-Gamo, Y. Sato, H. Kanda, *Diam. Relat. Mater.* **7**, 1719 (1998).
40. M. Mermoux, B. Marcus, G.M. Swain, J.E. Butler, *J. Phys. Chem. B* **106**, 10816 (2002).
41. S. Szunerits, M. Mermoux, A. Crisci, B. Marcus, P. Bouvier, D. Delabouglise, J.-P. Petit, S. Janel, R. Boukherroub, L. Tay, *J. Phys. Chem. B* **110** 23888 (2006).
42. K.B. Holt, A.J. Bard, Y. Show, G.M. Swain, *J. Phys. Chem. B* **108**, 15117 (2004).
43. H.V. Patten, K.E. Meadows, L.A. Hutton, J.G. Iacobini, D. Battistel, K. McKelvey, A.W. Colburn, M.E. Newton, J.V. Macpherson, P.R. Unwin, *Angew. Chem. Int. Ed.* **51**, 7002 (2012).
44. Y.-G. Lu, S. Turner, J. Verbeeck, S. Janssens, P. Wagner, K. Haenen, G. Van Tendeloo, *Appl. Phys. Lett.* **101**, 041907 (2012).
45. M.N. Latto, G. Pastor-Moreno, D.J. Riley, *Electroanalysis* **16**, 434 (2004).
46. M.C. Granger, G.M. Swain, *J. Electrochem. Soc.* **146**, 4551 (1999).
47. J.A. Bennett, J. Wang, Y. Show, G.M. Swain, *J. Electrochem. Soc.* **151**, E306 (2004).
48. K. Miyata, K. Kumagai, K. Nishimura, K. Kobashi, *J. Mater. Res.* **8**, 2845 (1993).
49. T. Watanabe, T.K. Shimizu, Y. Tateyama, Y. Kim, M. Kawai, Y. Einaga, *Diam. Relat. Mater.* **19**, 772 (2010).
50. M.C. Granger, J. Xu, J.W. Strojek, G.M. Swain, *Anal. Chim. Acta* **397**, 145 (1999).
51. H.B. Suffredini, V.A. Pedrosa, L. Codognoto, S.A.S. Machado, R.C. Rocha-Filho, L.A. Avaca, *Electrochim. Acta* **49**, 4021 (2004).
52. G.R. Salazar-Barda, L.S. Andrade, P.A.P. Nascente, P.S. Dizani, R.C. Rocha-Filho, L.A. Avaca, *Electrochim. Acta* **51**, 4612 (2006).
53. I. Duo, C. Levy-Clement, A. Fujishima, C. Comninellis, *J. Appl. Electrochem.* **34**, 935 (2004).
54. R.J. Rice, R.L. McCreery, *Anal. Chem.* **61**, 1637 (1989).
55. I.-F. Hu, D.H. Karweik, T. Kuwana, *J. Electroanal. Chem.* **188**, 59 (1985).
56. R. DeClements, T. Dallas, G.M. Swain, M.W. Holtz, R.D. Herrick, J.L. Stickney, *Langmuir* **12**, 6578 (1996).
57. J. Rusling, *ECS Interface* **18** (2), 34 (2009).
58. A. Heller, B. Feldman, *Chem. Rev.* **108**, 2482 (2008).
59. Y. Lee, J. Kim, *Anal. Chem.* **79**, 7669 (2007).
60. Y. Fang, E. Wang, *Chem. Commun.* **49**, 9526 (2013).
61. X. Niu, M. Lan, H. Zhao, C. Chen, Y. Li, X. Zhu, *Anal. Lett.* **46**, 2479 (2013).
62. D. Shin, B.V. Sarada, D.A. Tryk, A. Fujishima, J. Wang, *Anal. Chem.* **75**, 530 (2003).
63. K.L. Soh, W.P. Kang, J.L. Davidson, Y.M. Wong, A. Wisitsora-at, G. Swain, D.E. Cliffel, *Sens. Actuators B* **91**, 39 (2003).
64. A.P.P. Eisele, D.N. Clausen, C.R.T. Tarley, L.H. Dall'Antonia, E.R. Sartori, *Electroanalysis* **25**, 1734 (2013).
65. D.T. Shin, D.A. Tryk, A. Fujishima, A. Merkoci, J. Wang, *Electroanalysis* **17**, 305 (2005).
66. R. Hoffmann, A. Kriele, H. Obloh, J. Hees, M. Wolfer, W. Smirnov, N. Yang, C.E. Nebel, *Appl. Phys. Lett.* **97**, 052103 (2010).
67. P. Gan, R.G. Compton, J.S. Foord, *Electroanalysis* **25**, 2423 (2013).
68. C.E. Nebel, N. Yang, H. Uetsuka, E. Osawa, N. Tokuda, O. Williams, *Diamond Relat. Mater.* **18**, 910 (2009).
69. J.M. Halpern, S. Xie, G.P. Sutton, B.T. Higashikubo, C.A. Chestek, H. Liu, H.J. Chiel, H.B. Martin, *Diam. Rel. Mater.* **15**, 183 (2006).
70. J. Cvacka, V. Quaiserova, J.W. Park, Y. Show, A. Muck, G.M. Swain, *Anal. Chem.* **75**, 2678 (2003).
71. J. Park, V. Quaiserova-Mocko, B.A. Patel, M. Novotny, A.H. Liu, X.C. Bian, J.J. Galligan, G.M. Swain, *Analyst* **133**, 17 (2008).
72. J. Park, J.J. Galligan, G.D. Fink, G.M. Swain, *Anal. Chem.* **78**, 6756 (2006).
73. B.A. Patel, X. Bian, V. Quaiserova-Mocko, J.J. Galligan, G.M. Swain, *Analyst* **132**, 41 (2007).
74. J. Park, J.J. Galligan, G.D. Fink, G.M. Swain, *Auton. Neurosci.* **152**, 11 (2010). □



https://doi.org/10.1557/mrs.2014.94 Published online by Cambridge University Press